Automotive Experiences
Vol. 7 No. 3 (2024) pp. 389-405
p-ISSN: 2615-6202 e-ISSN: 2615-6636

Research Paper

Experimental and Finite Element Study of Rollover Protection Structure for a 22-Seat Man-hauler Superstructure Vehicle

Muchamad Gozali[1], Djoko Wahyu Karmiadji[1,2], Wina Libyawati[2], Budi Haryanto[1], Muhamad Masrur[1], Arief Setyawan[1], Wahyu Sulistiyo[1], Makmuri Nuramin[1], Anwar[1], Budi Susilo[3]

[1]Research Center for Structural Strength Technology, National Research and Innovation Agency, Tangerang Selatan 15310, Indonesia
[2]Department of Mechanical Engineering, Pancasila University, Jakarta Selatan 12640, Indonesia
[3]PT Bagong Dekaka Makmur, Indonesia

much001@brin.go.id (M.G); djok001@brin.go.id (D.W.K)

https://doi.org/10.31603/ae.11380

Published by Automotive Laboratory of Universitas Muhammadiyah Magelang

Article Info
Submitted: 15/05/2024
Revised: 28/09/2024
Accepted: 04/10/2024
Online first: 21/11/2024

Abstract

The application of man-hauler which classified as heavy-duty vehicle and operated on the upper ground mining, requires high safety measurement as arrange in the UN-ECE No. 66. The safety measure demands vehicles to undergo both structural testing and analysis. The investigation of structural testing for heavy-duty vehicles has been developed to the rollover testing that used tilting platform, to see the deformation impact toward the residual space and foresight opportunities for further development on the vehicle structure or warning system. Rollover testing is costly and time-consuming, so new or developed vehicle structure needs finite element model analysis, to predict the deformation level due to rollover incident. Both testing have the same goal which is to confirm the vehicle structure able to protect the passenger compartment. Therefore, this study aims to present a guidance to test a complete set of 22-seat man-hauler vehicle with stress distribution analysis, quasi-static loading test of body section, and tilting platform. The results of the stress distribution test are that the load is concentrated on the element number 148 in the rear UNP 100 profile. The results of the quasi-static loading test are that the maximum stress that occurs is 33% of the allowable stress. The simulation result under this condition shows that the maximum deflection value occurred in the side frame structure is 167.9 mm. The largest deformation due to the rolling test occurred at point E has a value of 27 mm located on the right side that experienced impact on the floor during the test. The overall testing and analysis can verify and confirm the vehicle structural strength, that the vehicle able to withstand the rollover impact and to protect the passengers.

Keywords: Rollover; Superstructure; Man-hauler; UN-ECE R66

1. Introduction

Safety issues in mining are crucial, especially for powered haulage equipment applications, such as the operation of man-hauler vehicles. The potential hazards in operating a man-hauler are accidents due to the fault interaction between equipment-to-equipment, equipment-to-human, and equipment-to-environment. Collisions between, losing control of vehicles, and overturning are the top accidents that cause occupational fatalities in the upper ground mining. Therefore, man-hauler applications in mining require further investigation, which covers equipment malfunction, environmental conditions, human errors, design failure, navigational failures, and overload [1].

High overturning cases of the man-hauler vehicle in mining and its similarity with medium-heavy duty bus characteristics, which uses a 4x4 driving system and superstructure body, lead to the man-hauler vehicle application must undergo

This work is licensed under a Creative Commons Attribution-NonCommercial 4.0 International License.

structure testing. The testing procedure refers to the UN-ECE Regulation No. 66 [2], [3]. The testing purpose is to verify that each passenger space in the vehicle experiences plastic deformation during impact or collision [4]–[6].

Heavy-duty vehicle handling on the off-road type, such as mining area contours, has been investigated for decades since it influences vehicle stability. Due to the expensive cost of conducting physical testing, the chorus of investigation transformed from physical to virtual testing. The virtual testing uses reliable design parameters and high-end multibody structure model simulation [7].

The stability test is mandatory for each batch of vehicle production and new vehicles to prove their safety level during on-the-road application. Rollover accidents are the worst result of unstable vehicle handling due to mishandling, landslides, or component failure. Cooperrider et al. [8] became a pioneer in investigating vehicle rollover behavior through the crash and dolly rollover experiment, and the investigation highlights the occurrence of constant trip force on a vehicle that resulted in the rollover of a vehicle. The experimental technique in mimicking the rollover accident for heavy-duty vehicles is developed continuously from comparing experiments with analytical results to observe the structure deformation [6], toward the sensor installation onto the tilting platform to monitor the injury level on the dummy placed inside the passenger space or know as residual space [9].

The comparison between experimental and virtual rollover testing results has a maximum 6.8% error, with the implementation of the neural network on the finite element model, Hong et al. [10] can control the relative error and can give recommendations of the allowable maximum bus mass by ECE R66 standard for side rollover. However, the model is set specifically for certain types of vehicles. Another comparison study was conducted by Choi et al. [11] to verify the analytical model of correlation between the center of gravity and static rollover angle, and the comparison study proposes a new static rollover angle model for single and double-axle vehicles with large errors for asymmetric vehicle, as well as new method to measure the center of gravity height by rotating the entire vehicle on the first axle. Farahani et al. [3] calculate the internal energy during rollover test from both experimental and finite element modelling, and the calculation result meets the UN ECE R66 standard regulation. Kepka et al. [12] conducted an experimental study to predict the rollover impact on the bus bodywork by testing part of the vehicle which represents joints, materials, and structure. The experimental result is set to build a virtual model for the bus structure. Davila and Martin [13] used partial part testing method to analyze the repaired body structure and to calculate average moment during deformation. The result of the partial testing shows loss mechanical properties of the part occurred when the repair altered the geometry, and the moment-angle curve of the repair part. The method to determine moment-angle curve can be extended to analyze plastic components in the vehicle with further material properties input in the finite element model. The overall experimental studies indicate the rollover test required development on the measurement method for the parameter related to center of gravity and the deformation indicator.

Chao et al. [14] propose an energy warning model in case of rollover for electric heavy-duty vehicle by implementing neural network, and model can predict the time to roll of a vehicle based on the three degree of freedom vehicle model during rollover. Chu et al. [15] also developed rollover speed prediction model based on the derivation of three-degree-of-freedom vehicle dynamics and lateral load transfer ratio (LTR) index is presented. The model is installed in the mobile phone for user friendly purposes and validated by using experiment. Guizhen et al. [16] purpose a real-time warning rollover model based on the road condition, and the warning model able to predict the lift off based on the applied velocity. An algorithm development is built by Li and Bei [17] to predict the occurrence of rollover because lateral velocity and high center of gravity, and the model able to predict the accidents ahead of the lift off situation and before the actual rollover occurred. Addisu et al. [18] and Karlinski et al. [2] develop finite element model for a vehicle based on quasi-static simulation to determine the energy absorbing and load-deformation behavior of the middle bus frame sections. Both studies result for different types of vehicles satisfy the requirement in UN-ECE R66. Those virtual studies above show rollover accidents can be estimated by analytical model with the machine learning implementation or by the application of finite element method. The five studies mentioned above do not discuss experimental residual space analysis and stress analysis due to loading. Therefore, this research completes critical areas for a more comprehensive understanding of previous research.

2. Research Objects and Method

2.1. *Research Objects*

The object of this study is a man-hauler unit with a 4x4 (4WD) front-rear drive system, see **Figure 1**. The man-hauler structure as the object of research is manufactured from JIS G3101 SS 400 structural steel or equivalent to ASTM A36 with a U-shaped profile and L profile connected with the welding process. The manufacturing process is carried out at PT. Bagong Dekaka Makmur, Malang. The man-hauler structure frame manufacturing process begins with the process of cutting the profile bar according to the size of the working drawing into small parts of the frame structure (section/member). The cutting area is then cleaned and flattened from uneven surfaces by grinding. The next stage is to combine the sections with the electric welding process so that it becomes the upper frame structure of the man-hauler. To ensure that there are no defects in the weld joint, a non-destructive test examination is carried out (Non-Destructive Test). The upper frame structure of the man-hauler is then placed on the Light Truck chassis which is fastened using brackets and several bolts and nuts.

The technical data of man-hauler are: Up to 22 passengers; Length: 4460 mm; Width: 2000 mm; Total load on frame: 3795 kg, with details: Body, Air Conditioning, Seats and accessories: 2115 kg; Passenger 22 persons: 1680 kg.

Figure 1. Man-hauler bus

2.2. *Methods*

Two activities were carried out in this study, namely:

a. Stress analysis of man-hauler structure, with finite element method approach. The purpose of this study is to determine the distribution of stress in the man-hauler structure due to normal load (normal load service).
b. Quasi-static loading test of body sections.
c. Man-hauler rolling test in complete condition with experimental methods referring to UN-ECE Standard R66. The purpose of this study was to determine the man-hauler structure capable of protecting the safety of passengers in the event of a man-hauler rollover accident.

3. Stress Analysis of Man-hauler Frame Structure

To comply with Indonesian Government Regulation (PP) Number 55 of 2012, the body frame that has been designed needs to be carried out engineering calculations to ensure the structure is in safe condition when bearing loads in the form of body, accessories, and passengers. So as a first step, a stress analysis of the man-hauler frame structure is carried out. The analyze was performed using the finite element method (FEM) computationally numerical with the help of CAE Nastran software.

The purpose of stress analysis is to obtain data in the form of stress values and maximum deformation that occur in the man-hauler frame structure with several variations in loading. The structure meets the safety criteria if the simulation results of maximum stress in the element are still below the value of the material clearance stress. In addition, it also provides several recommendations related to the results of the analysis that has been carried out. The frame man-hauler (**Figure 2**) is made of JIS G3101 SS400 structural steel. The properties of this material are shown in **Table 1**.

Table 1. JIS G3101 SS400 mechanical properties [19]

Properties	Value
Density	7860 kg/m^3
Yield strength	245 MPa
Ultimate tensile strength	400 MPa
Modulus of Elasticity	190-210 GPa
Poisson ratio	0.26
Hardness	160 HB

Figure 2. Man-hauler frame structure

Man-hauler frame body structure modeling is carried out with a bar element model (Figure 3) with material input following the data above, while input properties follow existing frame conditions with rectangular tube, U-shaped, and L-profile shapes. The sizes used are rectangular tubes measuring 80 x 40 mm (thickness 3.5 mm), 40 x 40 mm (thickness 2.5 mm), U-shaped profile 100 (size 100 mm x 50 mm), and L profile 40 (size 40 mm x 40 mm). The stress analysis of the man-hauler truss structure was carried out using Nastran software in the form of bar elements, each of which has its properties input according to its actual profile. The meshing process is carried out manually, namely one element for one section of the truss profile. To ensure that each part or element is connected perfectly, a join process between nodes or merge coincident nodes is carried out. The location of the load constraint is in the middle lower frame which is attached to the light truck chassis frame using several brackets and bolts. Meanwhile, loads in the form of side plates, roof, glass, floor plates, seats, passengers and other accessories are input on each element based on their placement location as shown in Figure 5.

Stress Analysis is carried out with maximum static loading conditions in the form of body weight, accessories, and passengers. Loading is performed on each frame node (Figure 4) which is inputted according to the weight of the load that is concentrated at that location. Loading on the frame (Figure 4) is carried out under the following conditions: Dead load condition; Dead load and Body combination; Combination of Dead load, Body, and Passenger.

Dead load condition loading is a frame condition without external loading or the frame is simulated with its gravity load. The loading of the dead load and body combination is a frame simulation with a combination of the frame load itself plus the body load in the form of a 1.2 mm thick body plate load, floor plate load, glass load, chair load, and accessories loads such as fans, stairs, and others. The loading of the combination of dead load, body, and passenger is with the previous combination load plus a passenger load of 22 peoples assuming the weight of each person

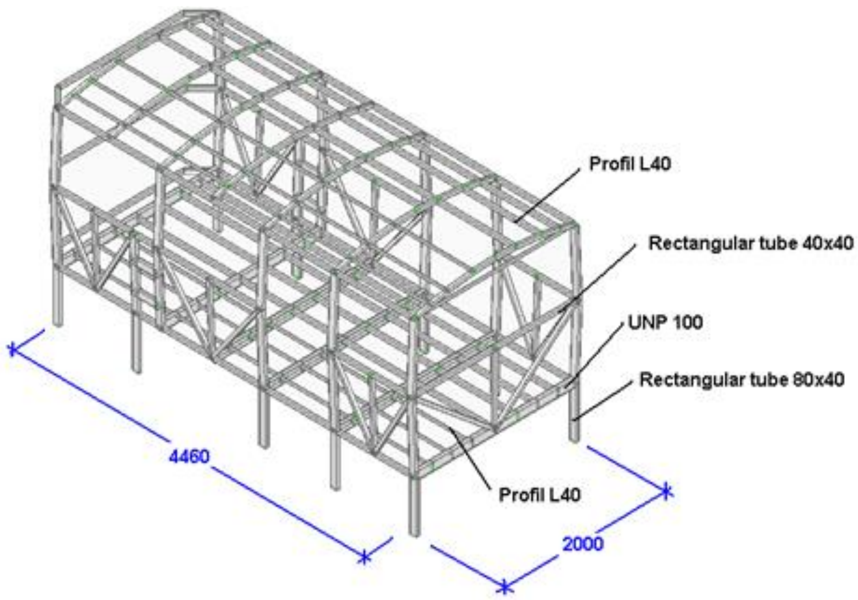

Figure 3. Bar element model of man-hauler frame

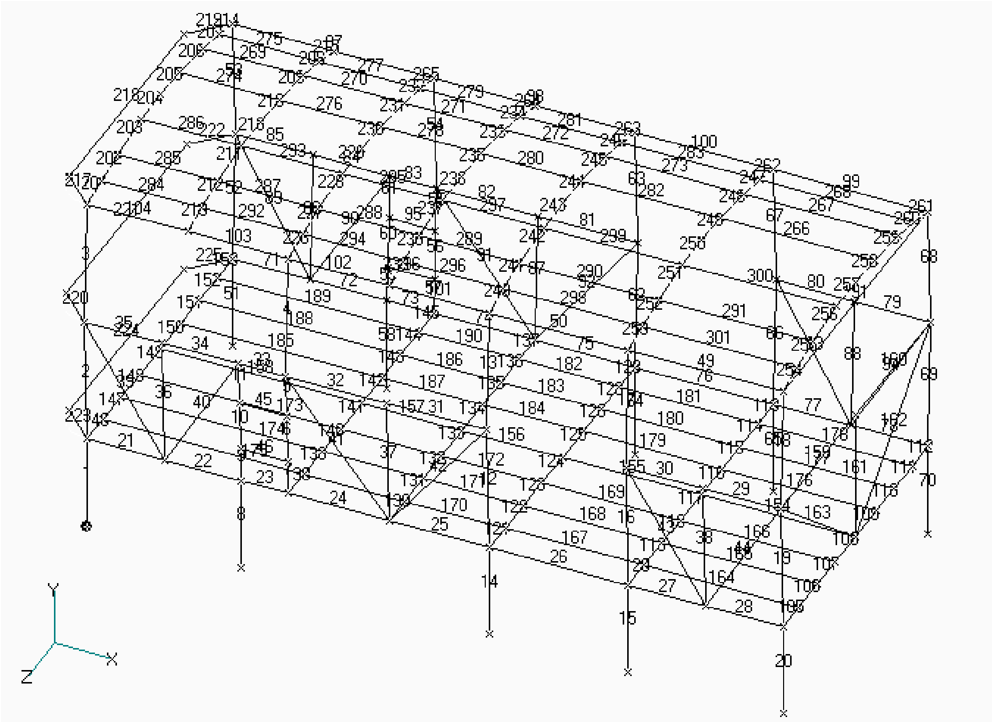

Figure 4. Identify of bar elements

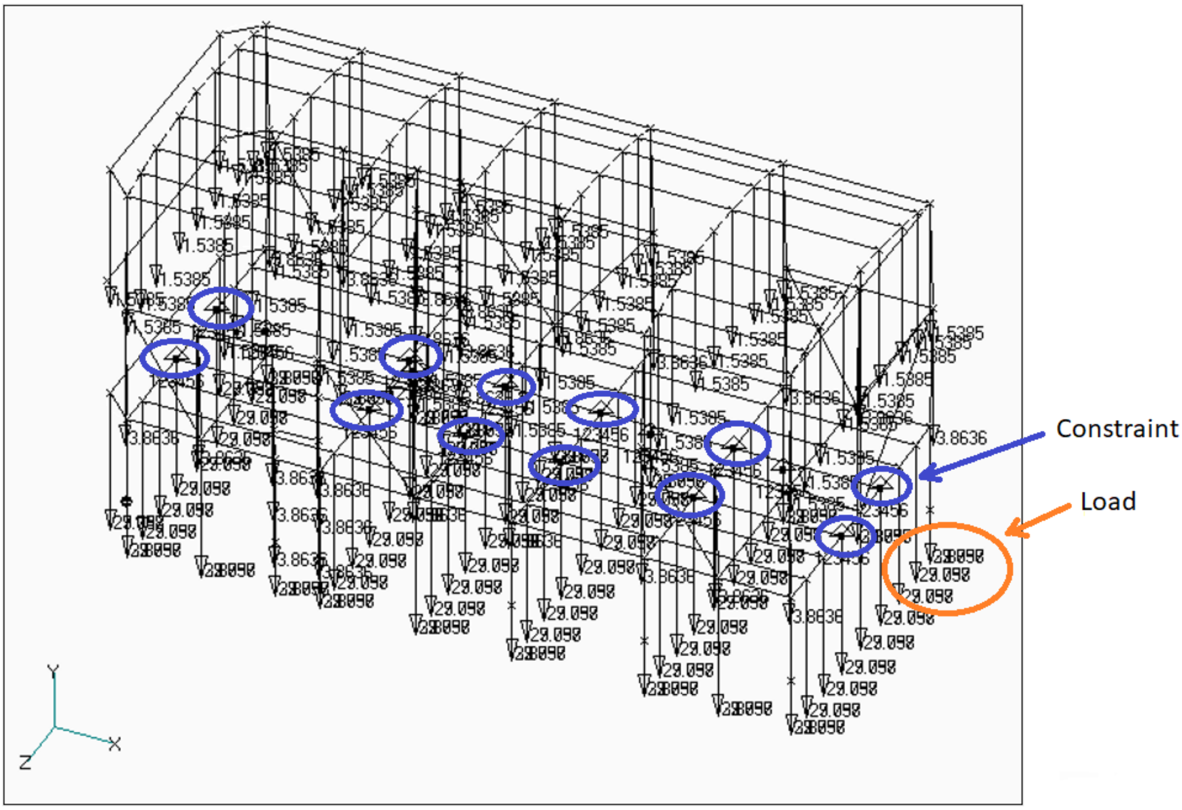

Figure 5. Load and constraint applications on bar elements

is 80 kg. The load constraint or load fulcrum with a fixed type is located on the UNP 100 profile which directly rests on the vehicle chassis fastened with bolt connections.

From the results of the FEM simulation by using Nastran, the value of the stress distribution that occurs is obtained, with several combinations of loading in **Figure 6** to **Figure 8**.

These explain the results of computational simulations where the stress distribution value that occurs in the bar element with dead load conditions with the highest stress value is 9.81 MPa which is located on the lower front crossbeam frame. The maximum stress value in dead load and body load conditions is 36.2 MPa which is located in the same position. For the case of full loading consisting of dead load, body load and passenger load, the maximum stress value that occurs is 54.60 MPa which occurs in the same position, namely on the lower front crossbeam frame.

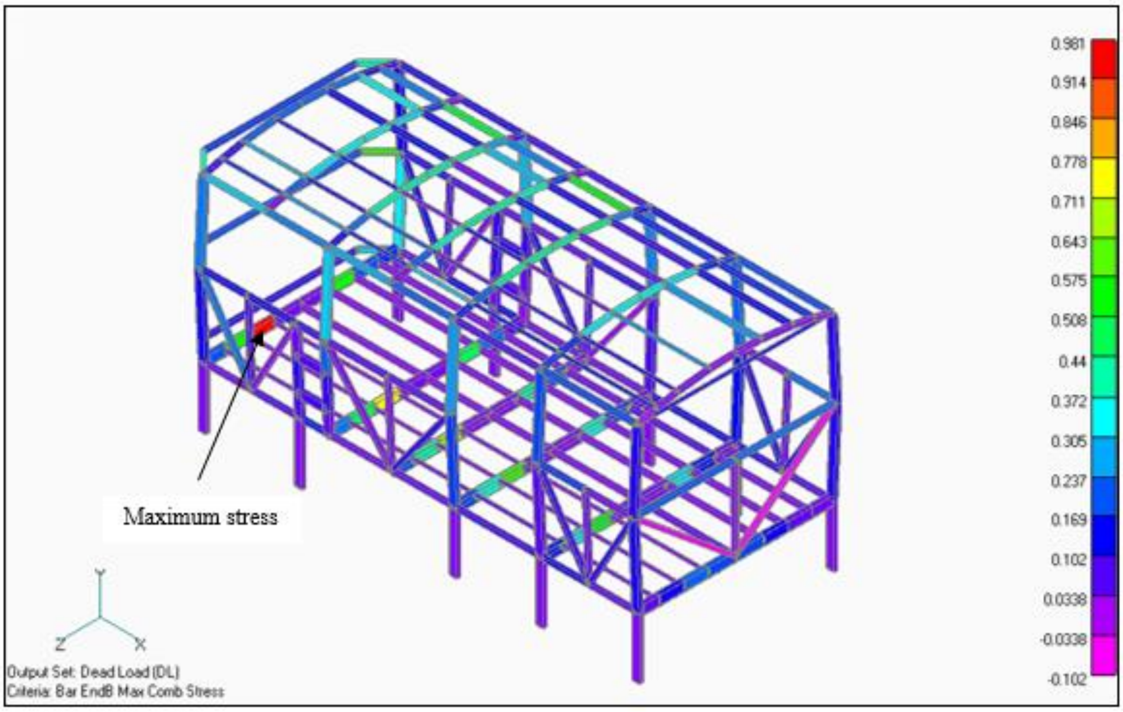

Figure 6. Stress distribution at dead load condition with a maximum stress value of 0.981 kg/mm^2 = 9.81 MPa

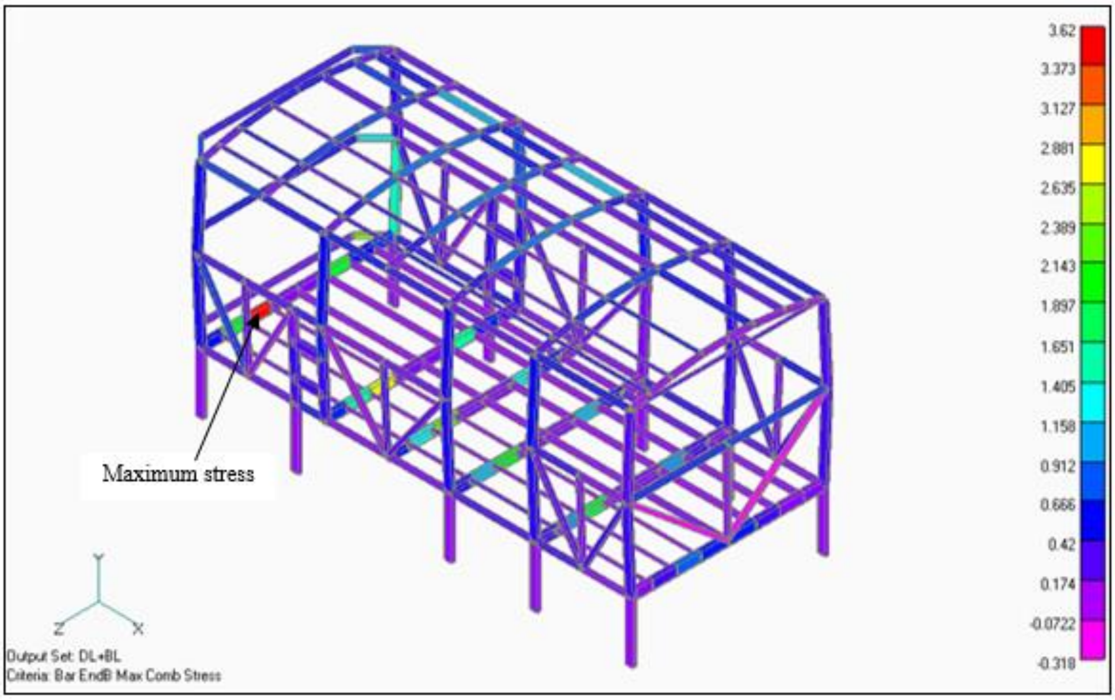

Figure 7. Stress distribution under dead load and body load conditions with a maximum stress value of 3.62 kg/mm^2 = 36.2 MPa

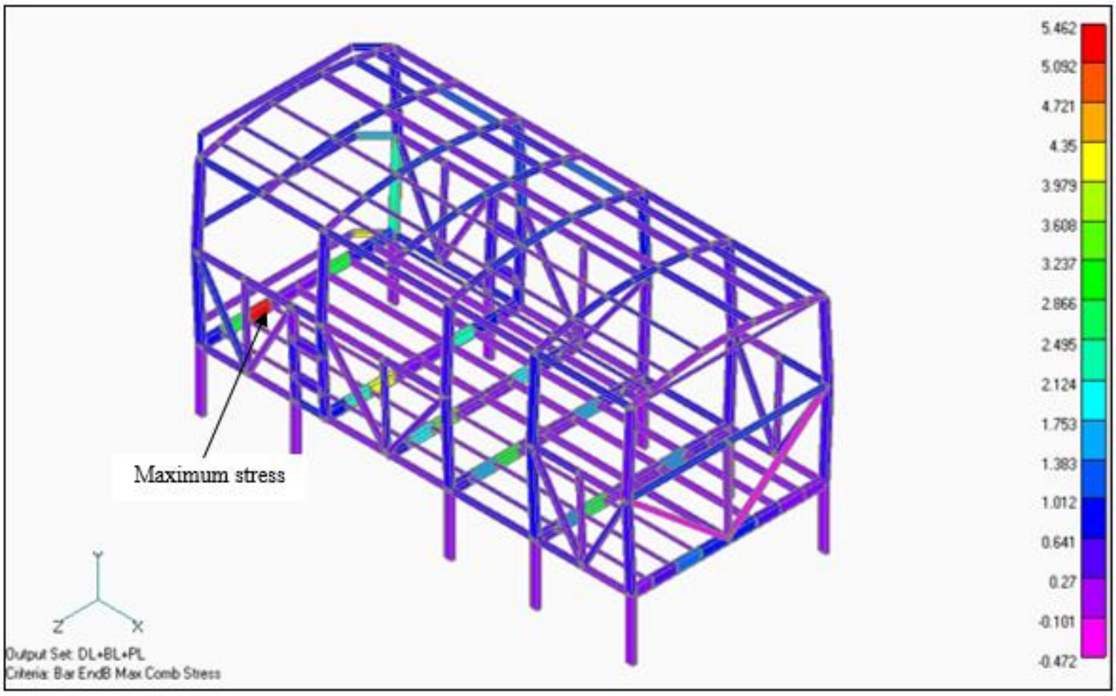

Figure 8. Stress distribution under dead load, body load, and passenger load conditions with a maximum stress value of 5.46 kg/mm^2 = 54.60 MPa

The main structure of the body in the form of a frame modeled according to actual conditions is simulated with the loads that converge on the frame in the form of body, glass, floor, passenger, and other accessories. The simulation results are evaluated against the stress value of the base material carbon steel JIS G3101 SS400 with characteristic of material are ultimate stress 400 MPa, yield stress 250 MPa and modulus elasticity 210 GPa. The maximum allowable stress is 2/3 of the yield stress of the material around 166.67 MPa [19]. These showed that the maximum stress value that occurred in the combination of dead load, body, and passenger loads of 5.46 kg/mm^2 was equivalent to 54.6 MPa which occurred in element number 148 in the rear UNP 100 profile. The maximum stress value that occurs is still below the allowable stress value with a ratio of 3.05. So numerical stress analysis can be concluded that the man-hauler frame structure is safe to withstand external loads.

4. Quasi-Static Loading Test of Body Sections

This quasi-static test uses the body section of the bus, which is carried out by pressing the cantrail of the bus structure (upper side frame) with a square pendulum. The load is distributed evenly on the cantrail, through a stiff beam, i.e. longer than the cantrail to simulate the floor in the rollover test. The direction of the applied load (see Figure 9) must correspond to the longitudinal direction of the vehicle's vertical center plane (VLCP) and its slope (α) is determined as follow Eq. (1) [20].

$$\alpha = 90\,° - \sin^{-1}\left(\frac{800}{H_c}\right) \tag{1}$$

where, H_c = cantrail height (in mm) of the vehicle measured from the horizontal plane where it stands.

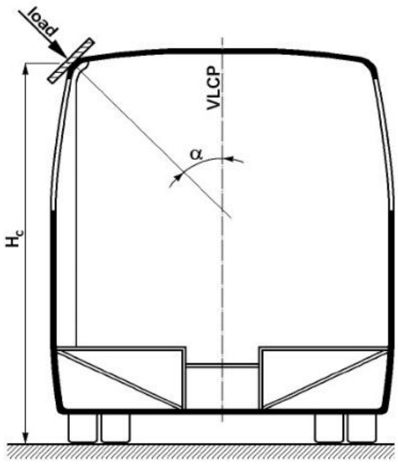

Figure 9. Load application on body section

The cantrail height value according to vehicle specifications (Hc) is 2780 mm, so the force angle obtained according to equation (1) is 73.3°. Static load models and simulations were created with Nastran software. An illustration of the application of loads to the model can be seen in **Figure 10**, and the simulation results are shown in **Figure 11**. According to UNECE R66 standard, the calculation of the total energy absorbed by the frame structure during the rollover test is:

$$E_T = 0.75 \times M \times g \times \Delta h \quad (2)$$

where, M = Vehicle mass (kg) = 4410.42 kg; g = Gravitational acceleration constant (m/s²) = 9.81 m/s²; Δh = Vertical displacement between the position of the vehicle's center of gravity (CoG) just before it leaves the platform and the position of the vehicle's center of gravity just before it hits the floor (m) = 1.82 m.

According to vehicle weight data, the highest CoG position of the vehicle when the platform rises and the CoG position of the vehicle just before hitting the ground (Δh) can be calculated by Nastran software with a value of 1820.04 mm. Through the impulse and momentum equations, the value of the static force applied to the vehicle model can be obtained from the impact speed value of the kinetic energy according to Eq. (3).

$$F = \frac{M \times v}{\Delta t} \quad (3)$$

where, F = static force (kN); v = speed at impact (m/s); Δt = time at impact (sec).

The speed value v is obtained from the relationship between kinetic and potential energy Eq. (2).

$$v = \sqrt{2}\, g\, h \quad (4)$$

The calculation results obtained a force value of 13414.12 kN assuming a Δt value of 0.2 seconds. This force is used as a static force in the finite element simulation as shown in **Figure 10**.

From the simulation results under these conditions (**Figure 11**), show that the maximum deflection value that occurs in the side frame structure is 167.9 mm. The distance between the frame and the residual space (point A) is 400 mm. Based on **Figure 11**, the deflection value at point A is 60.10 mm or about 15%.

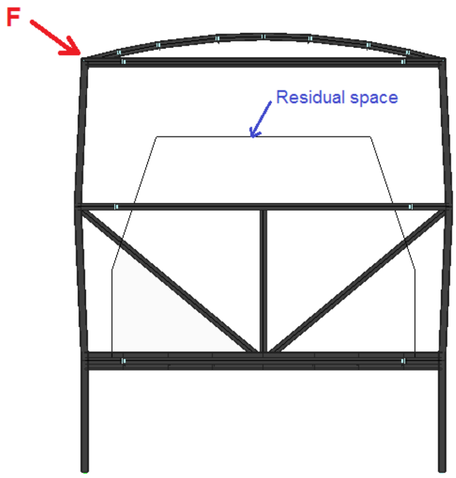

Figure 10. Application of load on the man-hauler frame body section model

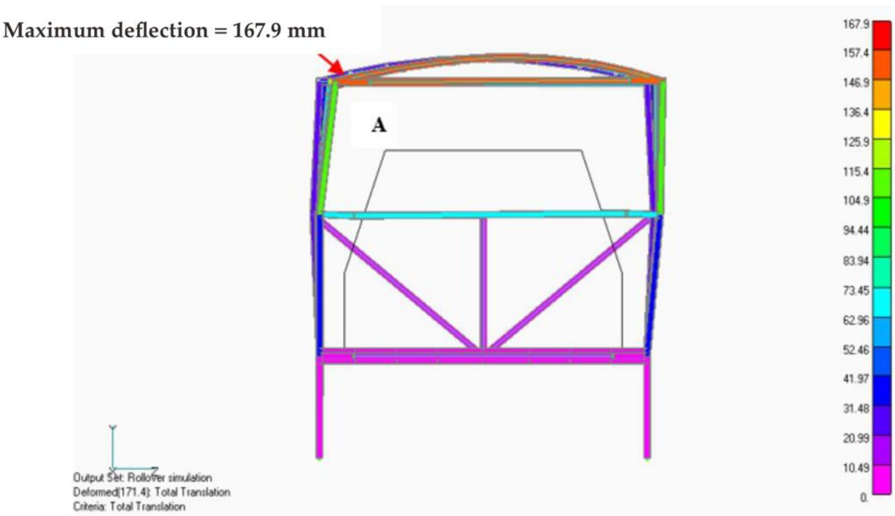

Figure 11. Simulation results of quasi static testing on the man-hauler frame body section model

5. Man-hauler Roll Test

The rolling test is a test on a vehicle by rolling the vehicle to prove the strength and durability of the superstructure based on standards. The UN-ECE R66 standard regulates the rolling tests to be carried out as well as the criteria that must be met by the bus superstructure. The superstructure of the bus has a direct influence on the protection of the lives and health of the passengers transported and guarantees the necessary living space in case of an accident. The rollover of the bus is very dangerous because it causes significant deformation of the roof and sidewalls. Generally, these standards are based on the importance of maintaining passenger safety. These standards state that the rolling test must follow the specifications and geometry of the platform slope as shown in **Figure 12** and **Figure 13**.

The rolling test based on the UN-ECE 66 standard is carried out following the following provisions [20].

5.1. Test Facility Preparation – Residual Space and Inclined Platform

The purpose of the international standard UN-ECE 66 is to ensure the effective protection of passengers and drivers in the residual space inside the bus during and after the vehicle rolls over. The specification of the residual space to be created is shown in **Figure 14** and **Figure 15**. All parts of the bus interior must be considered for their effect on residual space, for example, luggage storage located at the top left and right which can reduce the distance between residual space and body section. Then the height of the residual space with the floor needs to be increased according to the size of the trunk [20] The inclined platform is the equipment needed to lift the overturned vehicle. The platform must be rigid to support the vehicle and be able to move in a controlled manner with a maximum rotating speed of 5 degrees/second [20]. The specification of inclined platform dimensions is shown in **Figure 14** and **Figure 15**.

Test facility measurements have been carried out on inclined platforms (see **Figure 15**) and residual space (see **Figure 16** and **Figure 17**) to meet UN-ECE R66 standards. The inclined platform has met the standard dimensional specifications required by UN-ECE R66 as shown in **Table 2**. Man-hauler uses a 3-point seat belt so that the passenger dummy made of sand-filled sacks weighs 34 kg and is tied in such a way that it can stay on the seat during the rollover test process.

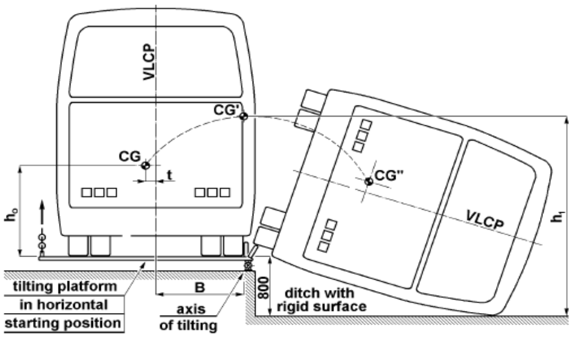

Figure 12. Rolling test specifications

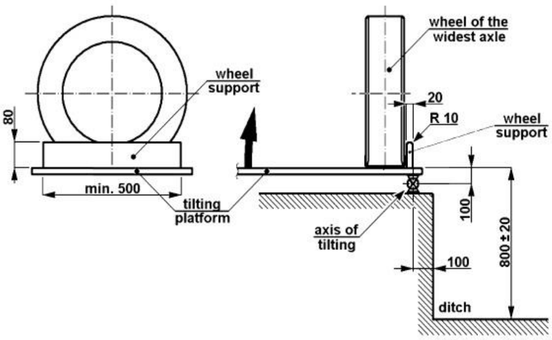

Figure 13. Inclined platform tilt geometry

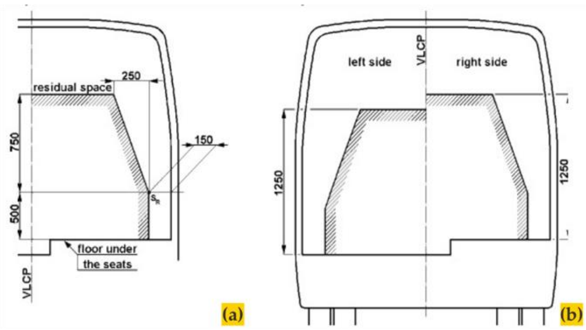

Figure 14. Specification of residual space lateral directional regulation

Figure 15. *Inclined platform*

Table 2. Inclined platform dimension measurement results

No.	Inclined Platform Parameters	Standard Geometry (Figure 11)	Inclined Platform Dimension(mm)	
			Front	Back
1	Platform height	800 ±20	794	798
2	Ditch-platform vertical distance	100	95	98
3	Ditch-platform horizontal distance	100	82	81
4	Tire support radius	10	10.06	13.1
5	Tire support thickness	20	20.12	26.2
6	Tire support length	Min. 500	502	575
7	Tire support height	80	80.1	84.47

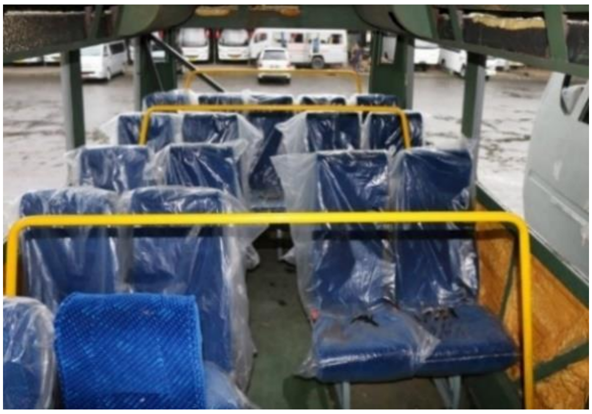

Figure 16. *Residual space* on man-hauler

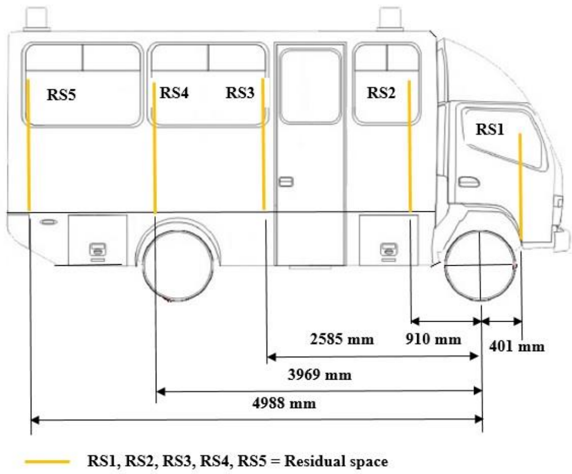

Figure 17. Position of *Residual space* on man-hauler

Some waterpass are installed on the inclined platform to record the angle of the platform when the vehicle rolls over and keep the angular velocity of the platform lift at the maximum limit of 5 degrees/s or 22.4 mm/s for the width of the inclined platform used in this test. The test used 4 units of High-speed cameras mounted on the front and rear of the man-hauler interior to record the condition of the residual space against the man-hauler frame, as well as the front and rear of the vehicle at a distance of about 2 meters outside the man-hauler to record the position of the Center of Gravity and also the condition of the residual space during the test.

5.2. *Preparation – Man-hauler*

The vehicle to be tested is prepared until it is ready for operation. Although the vehicle does not have to be in completely finished condition, it must be representative of a production vehicle with respect to unladen mass, center of gravity and mass distribution as stated by the manufacturer. Therefore, it is appropriate for every vehicle, especially manufactured products or body parts, to require data on the technical characteristics of the location of the vehicle's center of gravity which can be used as a reference when the vehicle is in operation, especially for used vehicles. by the general public both for transportation of goods and people [21]–[24].

Equipment and items used in the operation of the vehicle must be properly conditioned, such as the installation of devices that connect passengers to seats, closed doors and windows but not in an unlocked condition, and tire pressure according to specifications. Exceptions for safety reasons are allowed such as the release of flammable materials such as batteries or gasoline. Information such as total effective vehicle mass (unladen kerb mass + total occupant mass) and seat belt type must be provided before testing. This is related to the use of a dummy with a mass of 34 kg for a 3-point seat belt or 68 kg for a 2-point seat belt. The center of gravity of the dummy is arranged so that it is 100 mm above and ahead of the R points on the seat. The test must have at least 2 high-speed cameras mounted on the front and rear of the vehicle to observe residual space during the test. The dimensional conformity of the facility and man-hauler to applicable standards must be evaluated and recorded to ensure test quality. Man-hauler measures are evaluated against vehicle specifications during the design or manufacturing process, by checking several important components such as wheel pressure. length of the front wheelbase with the rear wheel (L), the distance between the midpoint of the front wheel (T1), the distance between the midpoint of the rear wheel (T2) **Figure 18**, and wheel radius (r). The results of man-hauler dimension measurements are shown in **Table 3**.

5.3. *Testing Process*

The vehicle is tested by stably and constantly lifting the tilted platform on the side opposite the pivot. The angular velocity of the platform lift is monitored so as not to exceed the maximum speed limit of 5 degrees/second as shown in **Figure 19**. Vehicle tires attach to the retaining plate so that the vehicle can roll over at the pivot point when the vehicle reaches the unstable equilibrium position. The test is stopped when the vehicle has rolled over until it touches the test floor. The damage caused to the post-test man-hauler was visually evaluated and recorded. The distance of the frame to the residual space is measured based on the marking points that have been given before the test. Measurement data is used as an evaluation of the acceptability of rollover testing.

6. Result and Discussion

Man-hauler rolling test with experimental method referring to UN-ECE Standard R66 is carried out on an open space with a concrete surface by lifting an inclined platform with a forklift. The platform is lifted at a speed not exceeding 5 degrees/sec (22.4 mm/s) to the equilibrium limit position of the structure. **Figure 20** and **Figure 21** show man-hauler before and after the rollover.

The condition of the residual space on the man-hauler after the rollover was recorded with two cameras with views on both sides: the front (**Figure 22** and **Figure 24**) and the rear of the structure (**Figure 23** and **Figure 25**).

To determine changes in superstructure due to vehicle rollover, measurements of structural dimensions are carried out in the residual space area before the rolling test and after the rolling test. Measurements are made from the position of the midpoint of the vehicle to the wall points of the structure (A, B, C, D, E, and O) as shown in **Figure 26**. Measurement of the marking beam distance from the vehicle floor was carried out at 6 points, namely at points A = 500 mm, B = 976 mm, C = 1076 mm, D = 1176 mm, E = 1250 mm, and O = 0 mm.

Figure 18. Vehicle dimension measurement

Table 3. Man-hauler dimension/specification

No.	Measuring Parameters	Measurement Results
1	Mass of empty Vehicle	4460 kg
2	Vehicle Mass + seat + dummy	5208 kg
3	Distance between front tires and rear tires (wheelbase)	3368 mm
4	Distance between 2 front tires	1492 mm
5	Distance between inner rear tires	1225 mm
6	Distance between outer rear tires	1764 mm
7	Tire Diameter	800 mm
8	Front tire pressure	940 psi
9	Rear tire pressure	920 psi

Figure 19. Forklift speed measurement for lifting platform

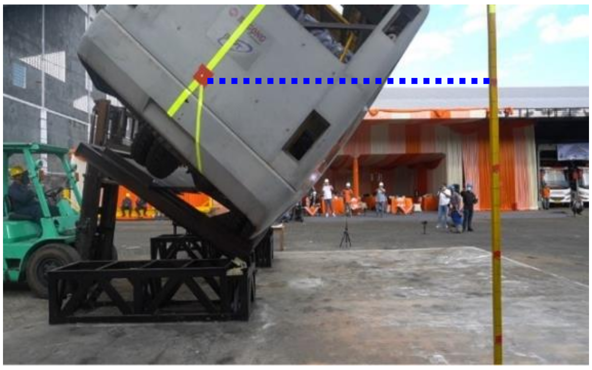

Figure 20. Man-hauler lifts before toppling with the Centre of Gravity at its highest point

Figure 21. The lowest position of the Centre of Gravity man-hauler after it toppled

Figure 22. Visual residual space against the vehicle wall right when the vehicle hits the floor seen from the front

Figure 23. Visual residual space against the vehicle wall right when the vehicle hits the floor seen from behind

Figure 24. Visual residual space against the vehicle wall right when the vehicle hits the floor seen from the outside of the front vehicle

Figure 25. Visual residual space against the vehicle wall right when the vehicle hits the floor seen from outside the rear of the vehicle

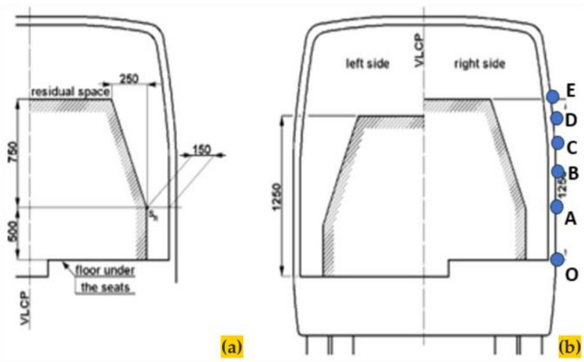

Figure 26. The position of the measurement points of the structure after the vehicle rolls over

The results of permanent deformation measurements performed after the test are shown in Figure 27 to Figure 30. Measurements were made at several points with various heights from the floor, namely points A (500 mm), B (976 mm), C (1076 mm), D (1176 mm), E (1250 mm), and O (0 mm). Measurements are made on the frame of the residual space as a reference which is assumed not to be deformed due to testing.

The measurement results of permanent deformation in the residual space of 2 are shown in Figure 27. The measurement results obtained the largest permanent deformation at point B of 10 mm. Figure 28 shows the measurement results in an area as far as 2585 mm from the front wheelbase in the longitudinal direction (residual space 3). From the picture it can be seen that the largest deformation occurred at point E of 27 mm, the deformation occurred on the right side, which is the side that experienced impact on the floor during the test. The direction of deformation is inward (towards the axis of the midline).

The deformation trend that occurs in the areas of residual space 4 (Figure 29) and 5 (Figure 30), shows a picture that is relatively similar to that of residual space 3. Maximum deformation occurs at point C in the area of residual space 4 of 19 mm, and residual space 5 of 15 mm. Deformation occurs on the side that experiences an inward impact (towards the lateral axis of the vehicle).

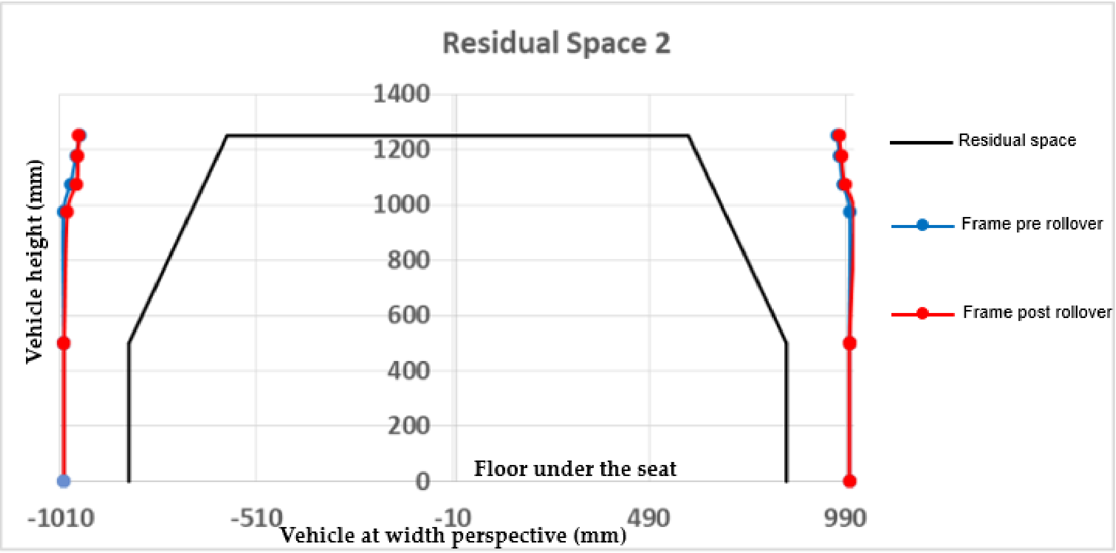

Figure 27. Dimensional measurement results in the residual area of space 2 before and after the roll test

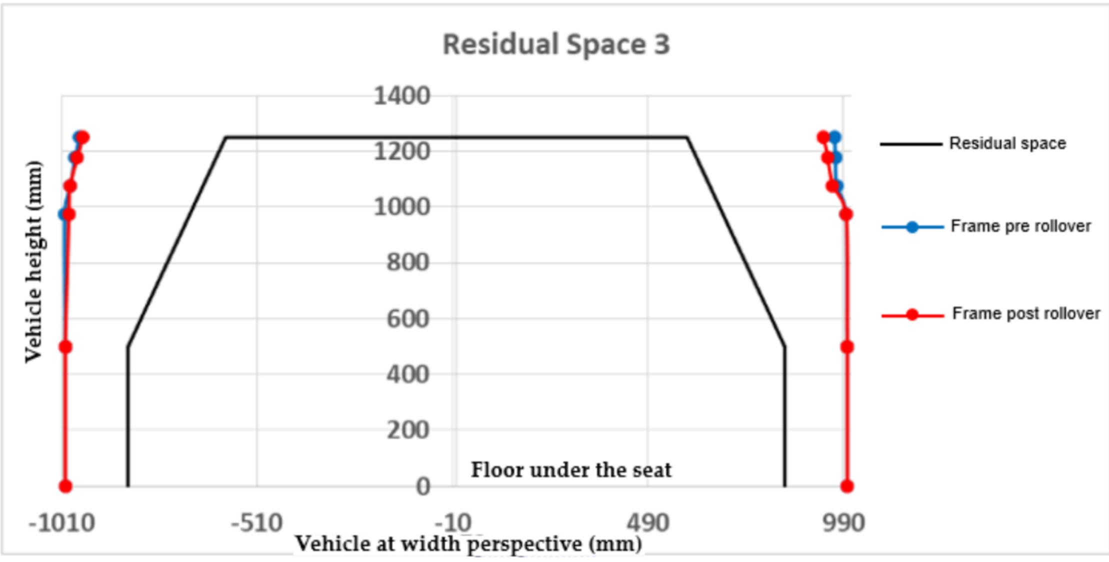

Figure 28. Dimensional measurement results in the residual space 3 areas before and after the roll test

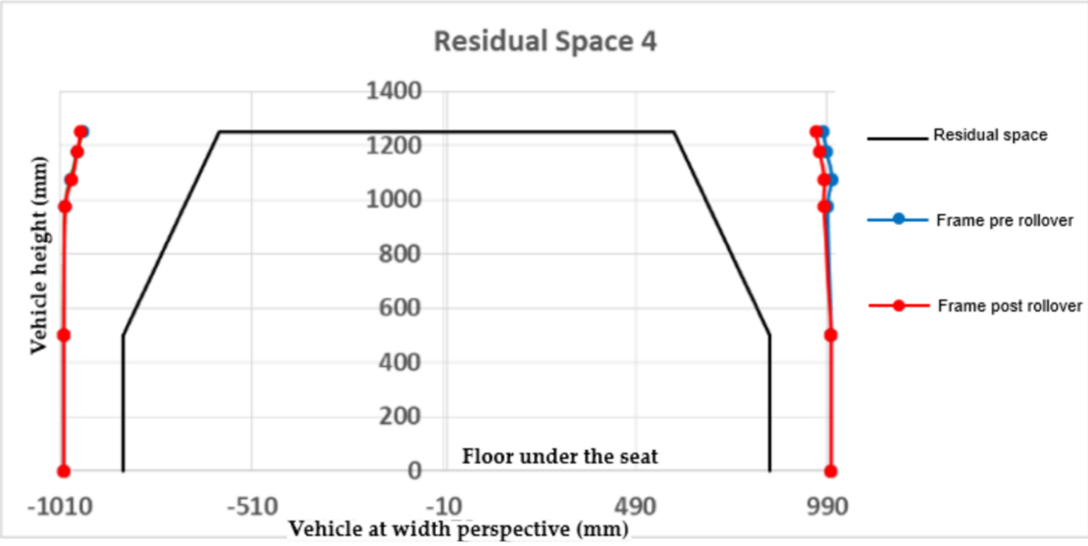

Figure 29. Dimensional measurement results in the residual area of space 4 before and after the roll test

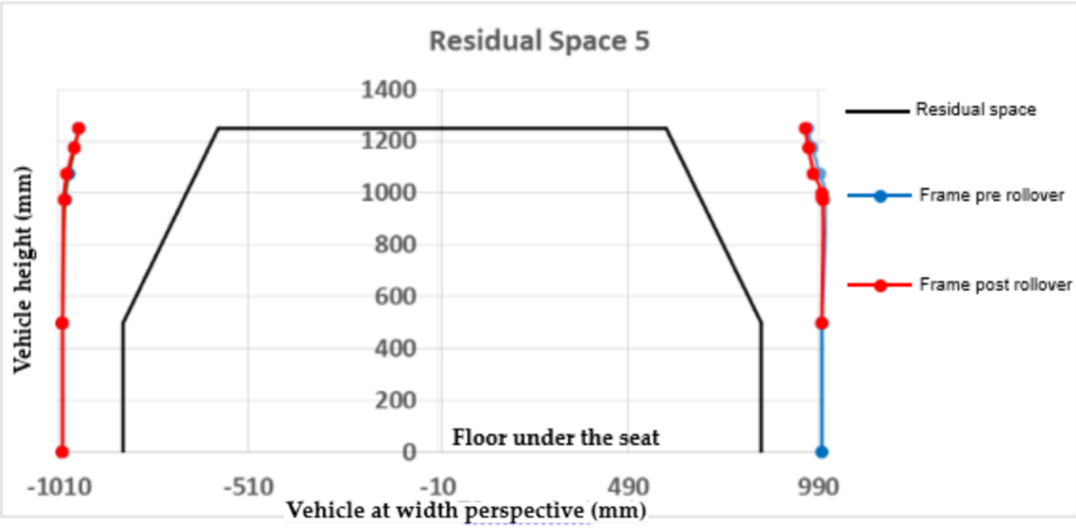

Figure 30. Dimensional measurement results in the residual space 5 areas before and after the roll test

Of the 4 locations where permanent deformation was measured (**Figure 27** to **Figure 30**), it showed that the deformation occurred on the side that had impacted the floor. The direction of deformation is towards the lateral axis point of the vehicle. While on the side that does not experience impact, deformation occurs relatively smaller.

Based on the residual space specifications shown in **Figure 11**, the distance between the lower residual space (point Sr) and the structure wall is 150 mm, and the distance between the upper residual space and the structure wall is 400 mm (point Sr + 250 mm)2), from the measurement results of permanent deformation that occurs relatively smaller or still far from the position of the residual space. Similarly, based on visual observations of all structures (pillars, cross sections, etc.) through the recording of the four cameras (**Figure 22** to **Figure 25**), it does not appear to touch or enter the residual space area after the roll. When the man-hauler touches the floor, the superstructure does not touch the residual space area as shown in **Figure 22** and **Figure 23**.

The rollover test research is intended to determine the energy due to impact and passenger safety, research on energy absorption has been discussed by previous researchers. This research on passenger safety is analyzed using residual space which is a safe space for passengers in the event of a collision.

The results of this study as shown in **Figure 27** to **Figure 30**, obtained a maximum deformation value of 27 mm at the location of point E residual space 3. The residual space limit between the frame and the residual space limit at point E is 373 mm, so the maximum deformation value that occurs is 6.75%.

7. Conclusion

Based on the numerical analysis results of the man-hauler frame structure, and from the results of experimental tests (rollover tests) on man-hauler it can be concluded that:

a. The maximum stress value that occurs due to normal load (normal service load) is 54.60 MPa, still below the material allowable stress value of 166.67 MPa.
b. Based on computational simulation, the maximum deflection of rollover test by using the quasi-static load is 167.9 mm, and at the location of residual space is 60.10 mm or 15 %. The maximum value of permanent deformation in the residual space under experimental *tests* occurs at point E residual space 3 around 27 mm or 6.75%. It shows this value is relatively small or far from the position of the residual space. The difference in value between computational simulation and experimental analysis is relatively small, namely 8.25%.
c. The visual observations of four camera resulted the walls of the structure do not appear to touch or enter the residual space area after the rolling test.

From the summary of the results of the numerical analysis of the man-hauler frame structure, experimental test results, and discussion, it can be concluded that the man-hauler superstructure is quite safe to use at its operating load and has adequate strength and rigidity to protect passenger safety in the event of a rollover man-hauler accident.

This study is limited to the object of man-hauler 4x4 for a capacity of 22 passengers, with a pillar structure of carbon steel material JIS G3101 SS400 in the form of a rectangular tube profile measuring 80x40 mm (thickness 3.5 mm), so that for the condition of man-hauler objects with different capacities and frame structures with different materials and shapes, further research is needed.

Acknowledgments

The authors would like to thank to National Research and Innovation Agency and PT. Bagong Dekaka Makmur, Malang for funding and collaboration in this research.

Author's Declaration

Authors' contributions and responsibilities

The authors made substantial contributions to the conception and design of the study. The authors took responsibility for data analysis, interpretation and discussion of results. The authors read and approved the final manuscript.

Funding

National Research and Innovation Agency.

Availability of data and materials

All data are available from the authors.

Competing interests

The authors declare no competing interest.

Additional information

No additional information from the authors.

References

[1] A. Moniri-Morad, M. S. Shishvan, M. Aguilar, M. Goli, and J. Sattarvand, "Powered haulage safety, challenges, analysis, and solutions in the mining industry; a comprehensive review," *Results in Engineering*, vol. 21, p. 101684, Mar. 2024, doi: 10.1016/j.rineng.2023.101684.

[2] J. Karliński, M. Ptak, P. Działak, and E. Rusiński, "Strength analysis of bus superstructure according to Regulation No. 66 of UN/ECE," *Archives of Civil and Mechanical Engineering*, vol. 14, no. 3, pp. 342–353, May 2014, doi: 10.1016/j.acme.2013.12.001.

[3] B. V Farahani *et al.*, "Passive Safety Solutions on Transit Buses: Experimental and Numerical Analyses," *Procedia Structural Integrity*, vol. 37, pp. 668–675, 2022, doi: 10.1016/j.prostr.2022.01.136.

[4] L. Kwaśniewski, J. Wekezer, B. Gepner, and J. Siervogel, "Development of simplified safety assessment procedure for paratransit buses," 2011.

[5] B. Gepner, C. Bojanowski, L. Kwasniewski, and J. Wekezer, "Effectiveness of ECE R66 and FMVSS 220 standards in rollover crashworthiness assessment of paratransit buses," *International Journal of Automotive Technology*, vol. 15, pp. 581–591, Jun. 2014, doi: 10.1007/s12239-014-0061-3.

[6] M. Seyedi, S. Jung, G. Dolzyk, and J. Wekezer, "Experimental assessment of vehicle performance and injury risk for cutaway buses using tilt table and modified dolly rollover tests," *Accident Analysis & Prevention*, vol. 132, p. 105287, Nov. 2019, doi: 10.1016/j.aap.2019.105287.

[7] M. El-Gindy and Z. El-Sayegh, "Vehicle Rollover Dynamics BT - Road and Off-Road Vehicle Dynamics," M. El-Gindy and Z. El-Sayegh, Eds. Cham: Springer International Publishing, 2023, pp. 185–230.

[8] N. K. Cooperrider, T. M. Thomas, and S. A. Hammoud, "Testing and Analysis of Vehicle Rollover Behavior," in *SAE Transactions*, Feb. 1990, vol. 99, pp. 518–527, doi: 10.4271/900366.

[9] D. A. Micu, M. D. Iozsa, and G. Fratila, "Experimental Test and Computer Simulation Research on Rollover Impact of a Bus Structure," 2014.

[10] H. C. Hong, J. Y. Hong, L. D'Apolito, and Q. F. Xin, "Optimizing Lightweight and Rollover Safety of Bus Superstructure with Multi-Objective Evolutionary Algorithm," *International Journal of Automotive Technology*, 2024, doi: 10.1007/s12239-024-00072-0.

[11] Y. H. Choi, K.-A. Kwon, and C.-H. Lee, "Experimental investigation on a static rollover angle model for commercial vehicle: new measurement method and theoretical model for double rear axle vehicle," *Journal of Mechanical Science and Technology*, vol. 36, no. 10, pp. 4943–4951, 2022, doi: 10.1007/s12206-022-0908-x.

[12] M. Kepka *et al.*, "Experiments to support the improvement of the integrity and resistance of the bus bodywork in a rollover accident," *Procedia Structural Integrity*, vol. 47, pp. 113–118, 2023, doi: 10.1016/j.prostr.2023.07.001.

[13] D. Rincón-Dávila, E. Alcalá, and Á. Martín, "Theoretical-experimental study of the repair of steel bus structures after rollover," *Journal of Constructional Steel Research*, vol. 162, p. 105734, Nov. 2019, doi: 10.1016/j.jcsr.2019.105734.

[14] P.-P. Chao, R.-Y. Zhang, Y.-D. Wang, H. Tang, and H.-L. Dai, "Warning model of new energy vehicle under improving time-to-rollover with neural network," *Measurement and Control*, vol. 55, no. 9–10, pp. 1004–1015, Aug. 2022, doi: 10.1177/00202940221113588.

[15] D. Chu, Z. Li, J. Wang, C. Wu, and Z. Hu, "Rollover speed prediction on curves for heavy vehicles using mobile smartphone," *Measurement*, vol. 130, pp. 404–411, Dec. 2018, doi: 10.1016/j.measurement.2018.07.054.

[16] Y. Guizhen, L. Honggang, W. Pengcheng, W. Xinkai, and W. Yunpeng, "Real-time bus rollover prediction algorithm with road bank angle estimation," *Chaos, Solitons & Fractals*, vol. 89, pp. 270–283, Aug. 2016, doi: 10.1016/j.chaos.2015.11.023.

[17] B. Li and S. Bei, "Research method of vehicle rollover mechanism under critical instability condition," *Advances in Mechanical Engineering*, vol. 11, no. 1, p. 1687814018821218, Jan. 2019, doi: 10.1177/1687814018821218.

[18] H. S. Addisu, E. G. Koricho, and A. A. Kassie, "Numerical Simulation and Optimization of a Locally Built Midibus Structure in Quasi-static and Rollover Condition," in *Artificial Intelligence and Digitalization for Sustainable Development*, B. H. Woldegiorgis, K. Mequanint, M. A. Bitew, T. B. Beza, and A. M. Yibre, Eds. Cham: Springer Nature Switzerland, 2023, pp. 95–126.

[19] Japanese Indurstrial Standard, *JIS G 3101:2015*. Japanese, 2015, p. 20.

[20] "Regulation No 66 of the Economic Commission for Europe of the United Nations (UN/ECE) — Uniform technical prescriptions concerning the approval of large passenger vehicles with regard to the strength of their superstructure." pp. 55–99, 2007.

[21] H. S. Hanandita, U. Ubaidillah, A. R. Prabowo, B. W. Lenggana, A. Turnip, and E. Joelianto, "Static Structural Analysis of Checking Fixture Frame of Car Interior Using Finite Element Method," *Automotive Experiences*, vol. 6, no. 3, pp. 652–668, 2023, doi: 10.31603/ae.9860.

[22] A. R. Zubir, K. Hudha, Z. A. Kadir, and N. H. Amer, "Enhanced Modeling of Crumple Zone in Vehicle Crash Simulation Using Modified Kamal Model Optimized with Gravitational Search Algorithm," *Automotive Experiences*, vol. 6, no. 2, pp. 372–383, Aug.

2023, doi: 10.31603/ae.9289.

[23] R. P. Putra, D. Yuvenda, M. Setiyo, A. Andrizal, and M. Martias, “Body City Car Design of Two Passengers Capacity: A Numerical Simulation Study,” *Automotive Experiences*, vol. 5, no. 2, pp. 163–172, 2022, doi: 10.31603/ae.6304.

[24] D. W. Karmiadji, M. Gozali, M. Setiyo, T. Raja, and T. A. Purnomo, “Comprehensive Analysis of Minibuses Gravity Center: A Post-Production Review for Car Body Industry,” *Mechanical Engineering for Society and Industry*, vol. 1, no. 1, pp. 31–40, 2021, doi: 10.31603/mesi.5250.